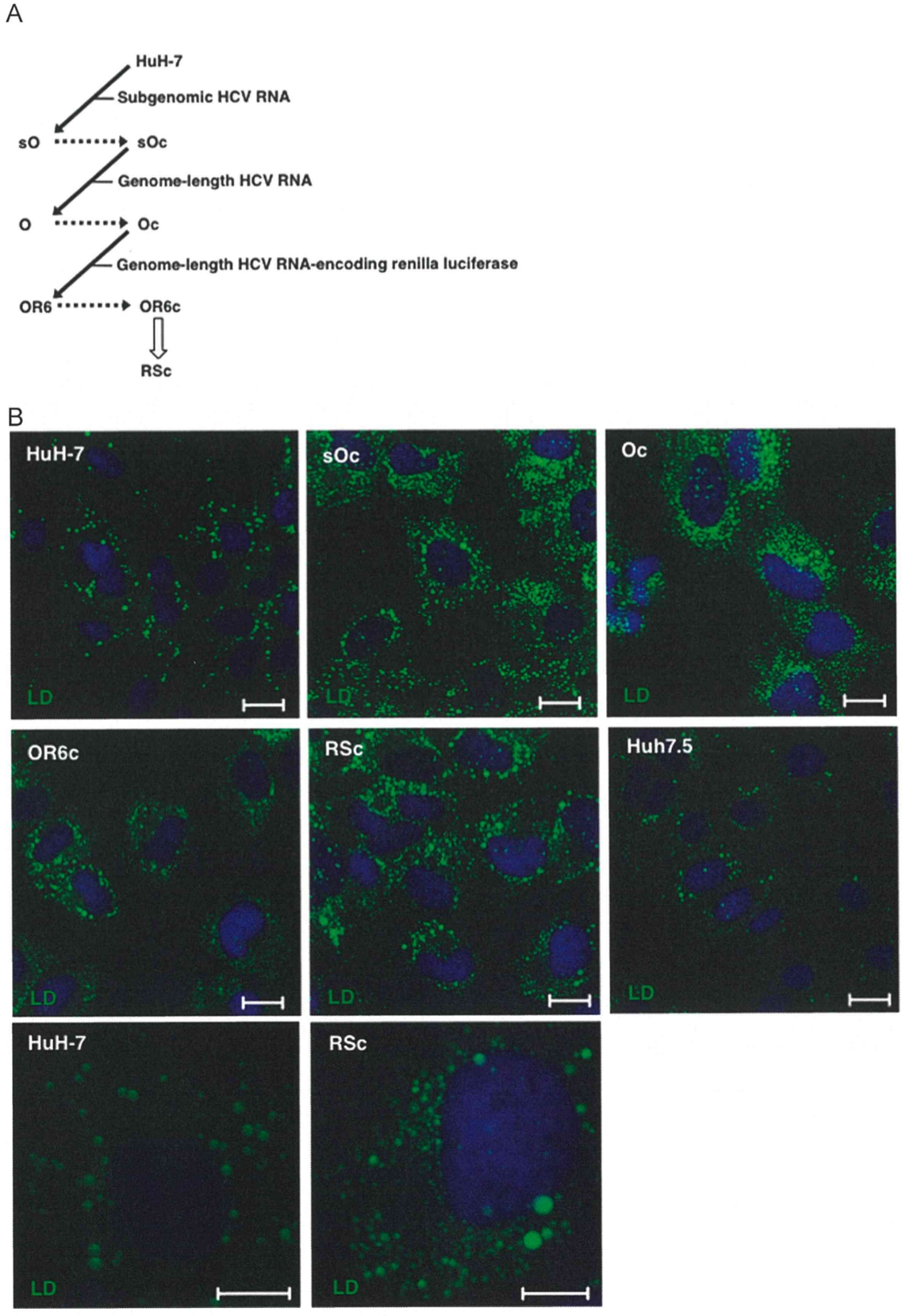

Fig. 1. RSc cells possess higher viral productivity in response to the infection with HCV-JFH-1 than Huh7.5 cells. (A) Outline for the establishment of our HCV RNA-replicating cells and their "cured" cells. Our HCV RNA-replicating cells (sO, O, and OR6 cells) are independently established by the transfection of HCV RNA into HuH-7 or cured cells (sOc or Oc cells) as previously reported (Ikeda et al., 2005, 2006; Kato et al., 2003). To prepare the cured cells, HCV RNA was eliminated from HCV RNA-replicating cells by the interferon treatment. RSc cells are one of the sublines of OR6c cells. The arrows with solid and dashed lines show the transfection of HCV RNA and the interferon treatment, respectively. (B) Visualization of LD under a confocal microscope. The panels show the fluorescence of LD by staining with BODIPY493/503. Bars, 20 μm. (C) Measurement of the mean fluorescence intensity of BODIPY493/503-stained cells by a flow cytometer. These levels were calculated relative to the level in HuH-7 cells, which was set at 1. (D) Quantitative RT-PCR analysis of HCV RNA in our cured cells 72 h after infection with HCV-JFH-1. Total RNA extracted from the cells was subjected to quantitative RT-PCR analysis. The experiments were performed in at least triplicate. (E) Time-course analysis of HCV RNA in RSc and Huh7.5 cells after infection with HCV-JFH-1. Total RNA was extracted from HCV-JFH-1-infected cells at each time point. (F) Quantitative RT-PCR analysis of HCV RNA in Huh7.5 cells 72 h after infection with intracellular (left panel) and extracellular (right panel) HCV-JFH-1. As intracellular or extracellular HCV-JFH-1, the lysate or the supernatant was recovered from RSc cells (designated J-RSc in the figure) and Huh7.5 cells (designated J-Huh7.5) 24 h after infection with HCV-JFH-1.

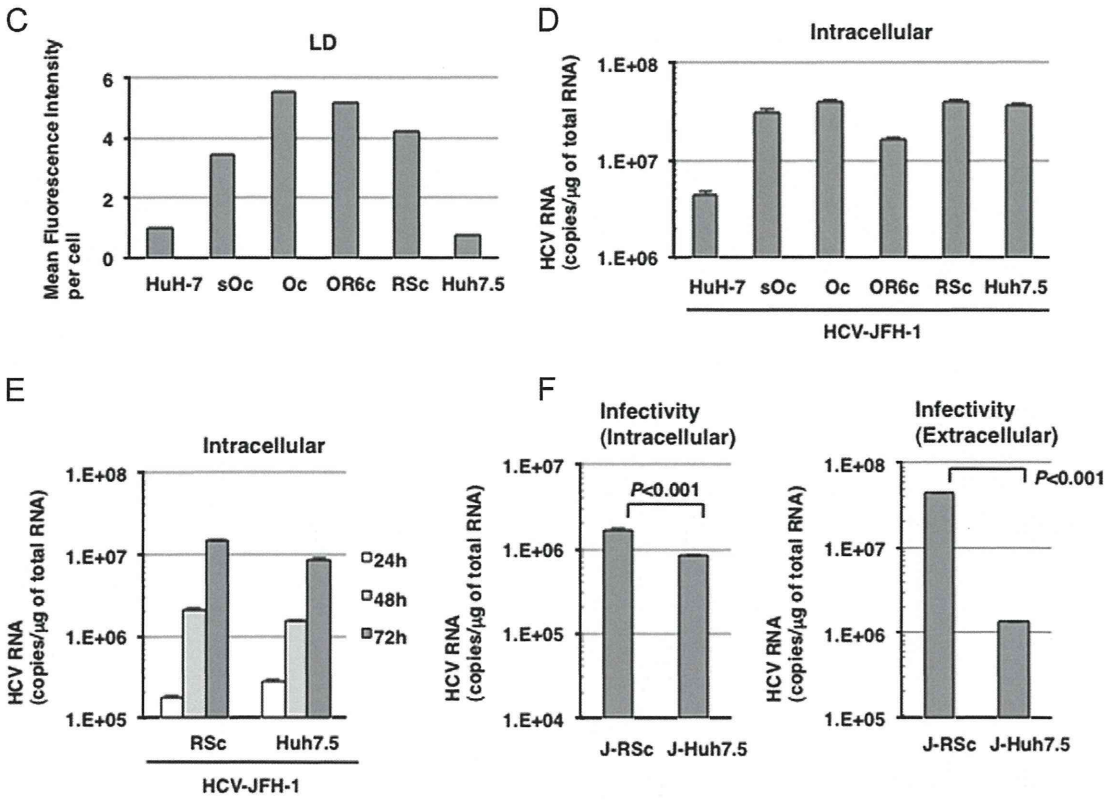

Fig. 1. (*continued*)

was co-localized with the core protein in HCV-JFH-1-infected RSc and Huh7.5 cells (Fig. 3A). We previously reported that the core protein was not recruited to LDs in O cells, from which no infectious virus was produced (data not shown). In fact, in contrast to HCV-JFH-1-infected RSc and Huh7.5 cells, co-localization of Rab18 and the core protein was not observed in O cells (Fig. 3B), although the expression of Rab18 were almost comparable levels among these cell lines (Supplemental Fig. S1C). We next examined the infectivity of intracellular viral particles in HCV-JFH-1-infected RSc siRab18 cells. The results revealed that the knockdown of Rab18 inhibited 90% of the production of intracellular viral particles (Fig. 3C) and the recruitment of the core protein to LDs (Fig. 3D). However, the knockdown of Rab4 (early endosome marker), other Ras-related small GTPase family member, inhibited only 40% of the production of intracellular viral particles (Supplemental Fig. S3C). These results suggest that Rab18 is particularly required for viral assembly through the trafficking of the core protein to LDs. Rab18 may be involved in the maturation of viral particles through membrane trafficking of the core protein from the ER to LDs.

Discussion

Previous proteomics analysis showed that a number of host factors were associated with LDs (Brasaemle et al., 2004). These LD-associated proteins may be required for the life cycle of HCV as well as the metabolism of lipids. During viral production, the HCV core protein is recruited to LDs in HCV-JFH-1-infected cells (Miyanari et al., 2007). In the present study, we suggest that one of the LD-associated proteins, Rab18, is required for trafficking of the HCV core protein to LDs and subsequent viral assembly.

The HCV core protein consists of three domains (domains 1, 2, and 3). Domain 2 (aa 118–173) contains two proline residues at aa positions 138 and 143, and a YATG sequence ranging from aa positions 164–167 that is essential for the association with LDs (Hope et al., 2002). These are conserved in both the JFH-1 strain (genotype 2a) and O strain (genotype 1b). However, the core protein was associated with LDs in HCV-JFH-1-infected RSc cells (Fig. 3D), but not in genome-length HCV RNA-replicating O cells (Kato et al., 2009). Matto et al. found that there were two morphologically distinct populations of the core protein (the ring-like and the dot-like pattern) in genome-length HCV RNA (genotype 1b)-replicating cells (Matto et al., 2004). The ring-like core protein was associated with LDs, and the dot-like core protein was associated with the detergent-resistant membranes and the lipid rafts essential for viral replication (Matto et al., 2004). We previously demonstrated that the core protein of the O strain showed a dot-like pattern (Kato et al., 2009), and that infectious virus was not produced from O cells (data not shown). In contrast to the core protein of the JFH-1 strain, the core protein of the O strain was not trafficked to LDs, and may have remained at the detergent-resistant membranes and the lipid rafts.

We also demonstrated that the core protein was co-localized with Rab18 in HCV-JFH-1-infected RSc cells, but not in O cells (Fig. 3B). In addition, we demonstrated that the knockdown of Rab18 did not inhibit HCV RNA replication in O cells as well as HCV-JFH-1-infected RSc cells (Supplemental Figs. S1B and S3B). However, in contrast to our results, Salloum et al. have previously observed that the knockdown of Rab18 inhibited HCV RNA replication in OR6 cells (Salloum et al., 2013). From these results, we speculate the clonality of HuH-7 cells as one of causes of this discrepancy. On the other hand, it also remains the possibility that the induction of IFN-β by shRNA reduced HCV RNA replication. Kenworthy et al. has previously reported that the introduction of shRNA by lentiviral vector may induce IFN-β (Kenworthy et al., 2009). Rab18 knockdown cells in the Salloum's paper were generated by the introduction of shRNA using lentiviral vector. In addition, Rab18 overexpression did not enhance HCV RNA replication in OR6 cells (Salloum et al., 2013). Another proteomic analysis suggested that Rab18 is upregulated in the lipid raft fraction of

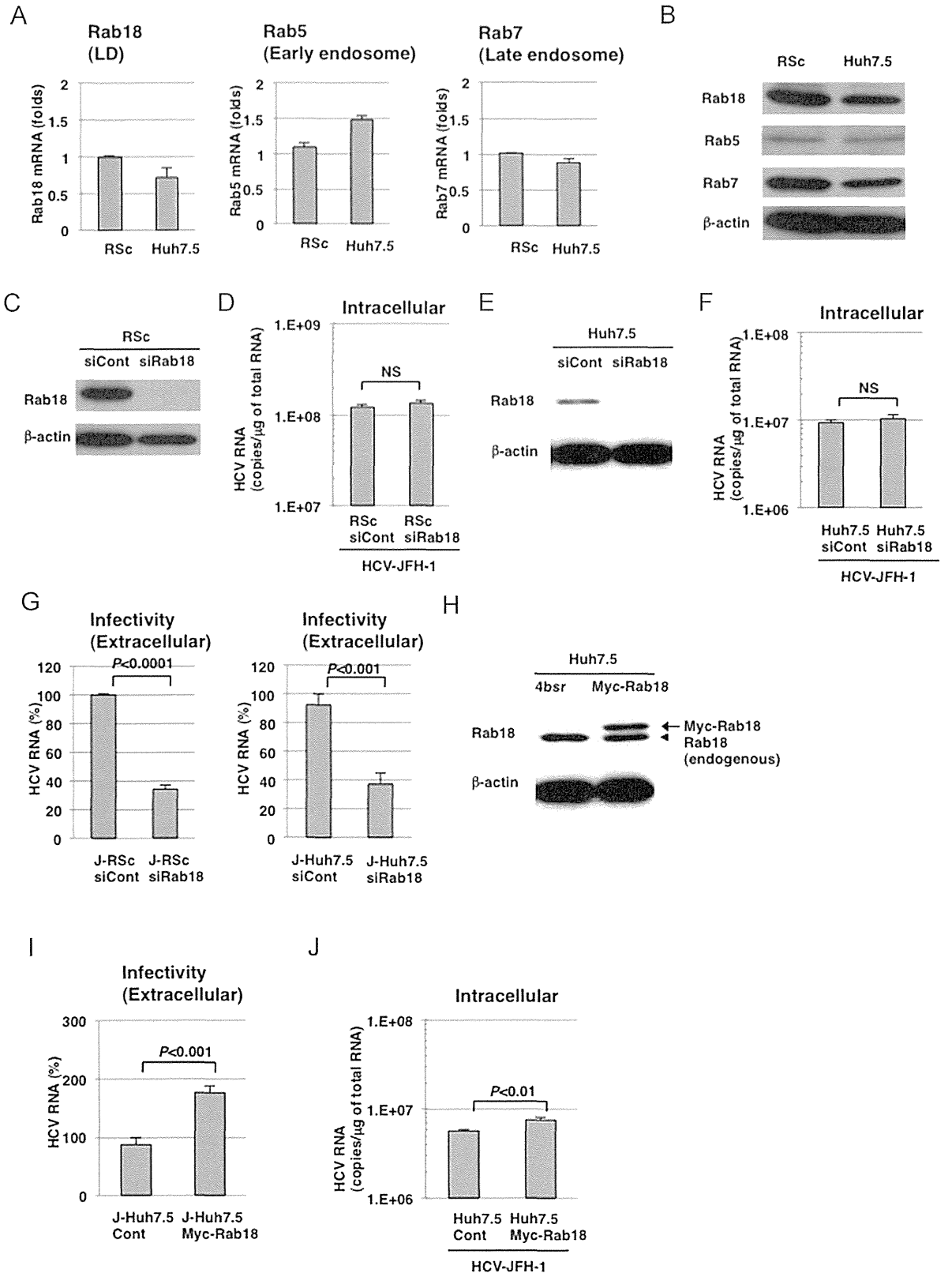

Fig. 2. Rab18 is required for viral production, but not viral RNA replication. (A) Quantitative RT-PCR analysis of Rab18, Rab5, and Rab7 mRNA in RSc and Huh7.5 cells. These levels were calculated relative to the level in RSc cells, which was set at 1. (B) Western blot analysis of Rab18, Rab5, and Rab7 in RSc and Huh7.5 cells. β-actin was included as a loading control. (C) Western blot analysis of Rab18 expression in RSc cells transfected with Rab18-specific (designated RSc siRab18 in the figure) or control (designated RSc siCont) siRNA. Cell lysates were prepared from RSc cells 120 h after transfection with Rab18-specific or control siRNA. (D) Quantitative RT-PCR analysis of HCV RNA in RSc siRab18 cells 24 h after infection with HCV-JFH-1. Transfection was performed 96 h before infection with HCV-JFH-1. NS: no significance. (E) Western blot analysis of Rab18 expression in Huh7.5 cells transfected with Rab18-specific (designated Huh7.5 siRab18) or control (designated Huh7.5 siCont) siRNA. (F) Quantitative RT-PCR analysis of HCV RNA in Huh7.5 siRab18 and siCont cells 24 h after infection with HCV-JFH-1. (G) Quantitative RT-PCR analysis of HCV RNA in Huh7.5 cells 72 h after infection with extracellular HCV-JFH-1. (Left panel) As extracellular HCV-JFH-1, the supernatant was recovered from RSc siCont cells (designated J-RSc siCont) or RSc siRab18 cells (designated J-RSc siRab18) 24 h after infection with HCV-JFH-1. (Right panel) The supernatant was also recovered from Huh7.5 siRab18 cells (designated J-Huh7.5 siRab18) and Huh7.5 siCont cells (designated J-Huh7.5 siCont) 24 h after infection with HCV-JFH-1. (H) Western blot analysis of Rab18 expression in Huh7.5 cells stably expressing Myc-tagged Rab18 (designated Huh7.5 Myc-Rab18). The arrow and arrowhead indicate exogenous (Myc-tagged) and endogenous Rab18, respectively. (I) Quantitative RT-PCR analysis of HCV RNA in Huh7.5 cells 72 h after infection with extracellular HCV-JFH-1. As extracellular HCV-JFH-1, the supernatant was recovered from Huh7.5 Cont (designated J-Huh7.5 Cont) or Huh7.5 Myc-Rab18 (designated J-Huh7.5 Myc-Rab18) 24 h after infection with HCV-JFH-1. (J) Quantitative RT-PCR analysis of HCV RNA in Huh7.5 Myc-Rab18 cells 24 h after infection with HCV-JFH-1.

genome-length HCV RNA (genotype 1b)-replicating cells (Mannova et al., 2006). These results may suggest that Rab18 also remained at the detergent-resistant membranes and the lipid rafts in the genome-length HCV RNA (genotype 1b)-replicating cells such as O cells. In addition, the gene silencing of Rab18 (Rab18-knockdown JFH-1-infected RSc cells) blocked localization of the HCV-JFH-1 core protein to LDs (Fig. 3D). Interestingly, the morphology of the population of HCV-JFH-1 core proteins was changed from a ring-like pattern to a dot-like pattern by the gene silencing of Rab18 (Fig. 3D). The HCV replication complex is formed on detergent-resistant membranes of the ER lumen (Shi et al., 2003). The ectopic expression of Rab18 induces the close apposition of LD to ER membranes through the reduction of ADRP (Ozeki et al., 2005). Rab18 may be one of the key host factors for the switch from the viral replication step to the viral assembly step through the close apposition of the detergent-resistant membranes to LDs. Rab18 may be an important target for the development of more effective anti-HCV reagents.

Materials and methods

Cell culture, reagents, and plasmids

Human hepatoma Huh7.5 cells were provided by Apath LLC (Brooklyn, NY). Huh7.5 cells, HuH-7 cells, and our established HuH-7-derived cells (sOC, Oc, OR6c, and RSc cells) were cultured in Dulbecco's modified Eagle's medium (Invitrogen, Carlsbad, CA) supplemented with 10% fetal bovine serum. Blasticidin (2 μg/ml) was used for the selection of Huh7.5 cells exogenously expressing Myc-Rab18. G418 (0.3 mg/ml) was also used for the selection of genome-length HCV RNA-replicating O cells.

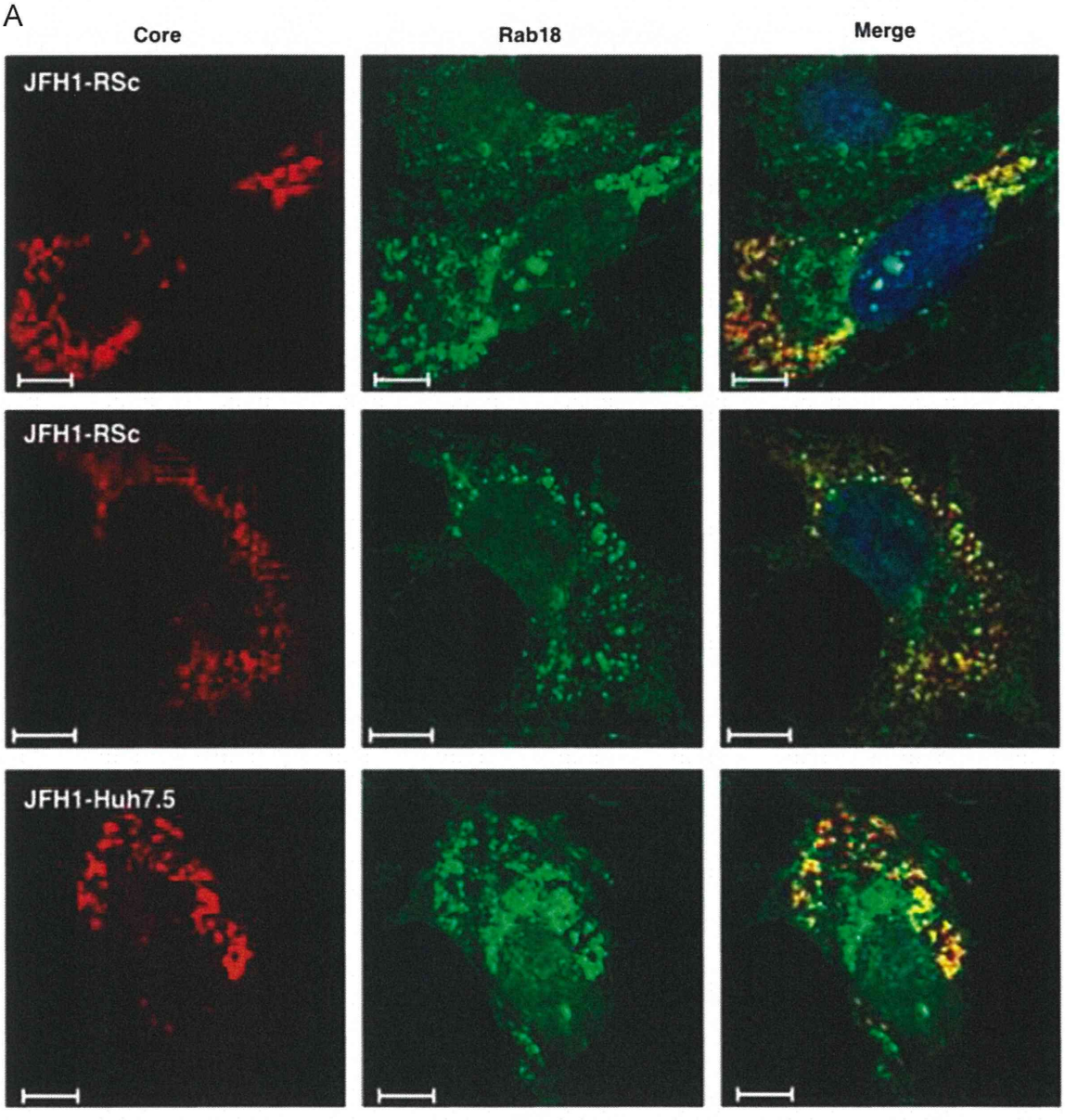

Fig. 3. Rab18 is required for viral assembly through the trafficking of HCV-JFH-1 core protein on LDs. (A) Visualization of the HCV-JFH-1 core protein (red) and Rab18 (green) under a confocal microscope. The panels show RSc or Huh7.5 cells 72 h after infection with HCV-JFH-1. Bars, 10 μm. (B) Visualization of the core protein (red) and Rab18 (green) in O cells. Bars, 10 μm. (C) Quantitative RT-PCR analysis of HCV RNA in Huh7.5 cells 72 h after infection with intracellular HCV-JFH-1. As intracellular HCV-JFH-1, the lysate was prepared from RSc siRab18 cells (designated J-RSc siRab18) and RSc siCont cells (designated J-RSc siCont) 24 h after infection with HCV-JFH-1. (D) Visualization of the HCV-JFH-1 core protein (red) and LD (green) under a confocal microscope. The panels show RSc siRab18 and siCont cells 72 h after infection with HCV-JFH-1. Bars, 10 μm.

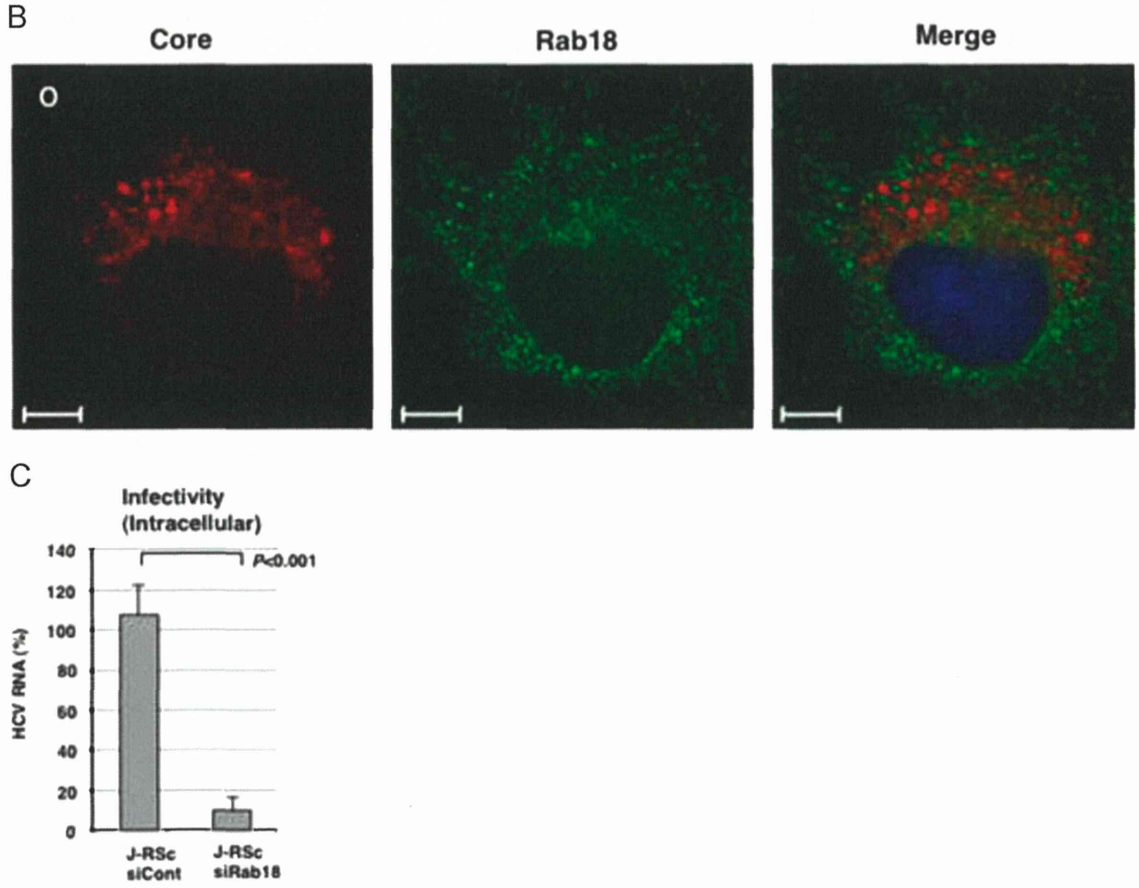

Fig. 3. (*continued*)

Immunofluorescence analysis

The LDs were stained with BODIPY493/503 (Invitrogen), and then photographed under a confocal microscope. Anti-Core antibody (CP11; Institute of Immunology, Tokyo, Japan) and anti-Rab18 antibody (Sigma, St. Louis, MO) were used as the primary antibodies. AlexaFluor 488-conjugated goat anti-rabbit antibody and AlexaFluor 594-conjugated goat anti-mouse antibody (Invitrogen) were used as the secondary antibodies. The intracellular localizations of HCV core protein and Rab18 were visualized and photographed under a confocal microscope as previously reported (Dansako et al., 2008). 4′-6-diamino-2-phenylindole (DAPI; Sigma) was used for visualization of the nucleus.

Flow cytometric analysis

The LDs were stained with BODIPY493/503 and then their mean fluorescence intensity was measured by a flow cytometer. The levels of LDs were calculated relative to the level in HuH-7 cells, which was set at 1.

Infection with HCV-JFH-1

The cells were infected with HCV-JFH1 (genotype 2a) for the appropriate time at a multiplicity of infection (MOI) of 1, and then the samples were prepared for the Western blot analysis, immunofluorescence analysis, and quantitative reverse transcription (RT)-PCR. Cell lysates and supernatants were prepared from the HCV-JFH-1-infected cells to monitor intracellular and extracellular infectivity. Intracellular HCV-JFH-1 was prepared from HCV-JFH-1-infected cells by repeated freeze-thaw cycles.

Generation of Rab18-knockdown cells

Small interfering RNAs (siRNAs) targeting Rab18 (Thermo Scientific; M-010824-00-0005) were prepared to generate Rab18-knockdown cells. siRNAs targeting Rab18 or non-targeting siRNAs (Thermo Scientific; D-001206-13-20) were introduced into RSc or Huh7.5 cells by DharmaFECT transfection reagent (Thermo Fisher Scientific, Waltham, MA). After transfection for the appropriate amount of time, Rab18-knockdown cells were infected with HCV-JFH-1.

Quantitative RT-PCR analysis

Total cellular RNA was isolated from HCV-JFH-1-infected cells by using an RNeasy mini kit (Qiagen, Hilden, Germany). RT was performed as previously described (Dansako et al., 2009). A SYBR Premix Ex Taq kit (TaKaRa Bio, Otsu, Japan) was used to measure the RNA levels of Rab18, Rab5, Rab7, GAPDH, or HCV. We used the following forward and reverse primer sets for quantitative PCR: for Rab18, 5′-GCGGAACGGGGTCAGGATGG-3′ (forward) and 5′-AAGAG CAGGCTGGACTTGCCC-3′ (reverse); for Rab5, 5′-GCTTGCTGCGGTCT CAGGTTTCT-3′ (forward) and 5′-TGGCCCGTTGGGTCTTGTTGC-3′ (reverse); for Rab7, 5′-CTCATCCAGGCCAGTCCCCGA-3′ (forward) and 5′–CCCGCTTTGTGGCCACTTGTC-3′ (reverse); for HCV and GAPDH, the primer sets are given in Dansako et al., 2013 and Dansako et al., 2003, respectively. The levels of Rab18, Rab5, Rab7, and HCV were normalized to the levels of GAPDH mRNA. The mRNA levels of Rab18, Rab5, and Rab7 in Huh7.5 cells were calculated relative to the level in RSc cells, which was set at 1. In vitro-transcribed HCV-JFH-1 RNA was used as the standard to calculate the amount of HCV RNA in HCV-JFH-1-infected cells. Data are the means ± SD from three independent experiments.

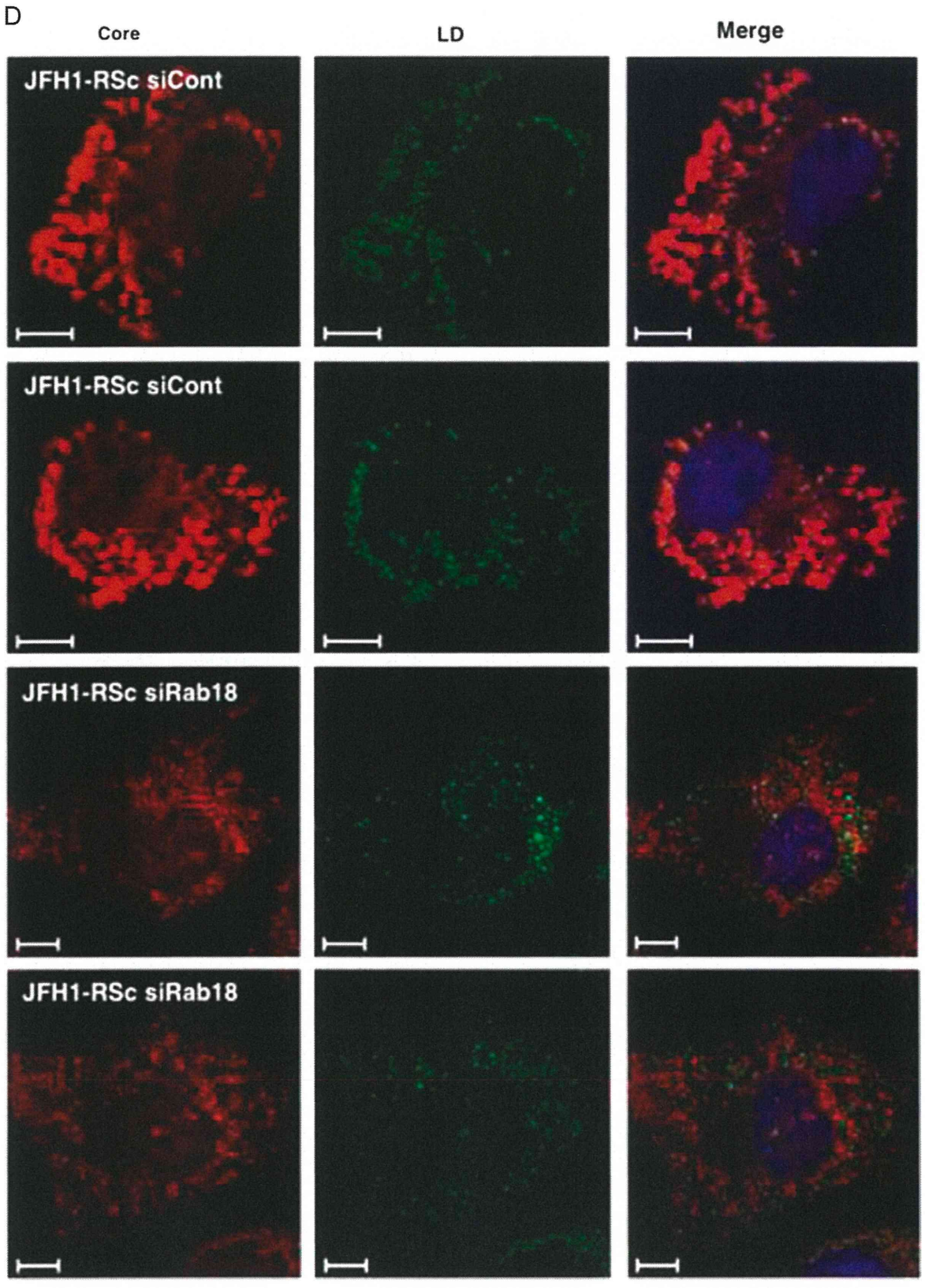

Fig. 3. (*continued*)

Western blot analysis

Preparation of cell lysates, and SDS-polyacrylamide gel electrophoresis were performed as previously described (Dansako et al., 2005). Gel was transferred to an Immobilon PVDF membrane (Millipore, Billerica, MA) by using a semi-dry transfer system: Horize BLOT 2MR (ATTO, Tokyo, Japan). Anti-Core (CP11; Institute of Immunology Co.), anti-Myc (PL14; Medical & Biological Laboratories, Nagoya, Japan), anti-Rab18 (Sigma), anti-Rab5 (S-19; Santa Cruz Biotechnology. Santa Cruz, CA), anti-Rab7 (Sigma),

and anti-β-actin antibody (AC-15; Sigma) were used in this study as primary antibodies. HRP-conjugated anti-mouse-IgG or anti-rabbit-IgG was used in this study as a secondary antibody (Cell Signaling Technology, Beverly, MA). Immunocomplexes were detected as previously described (Dansako et al., 2007).

Statistical analysis

Determination of the significance of differences among groups was assessed using the Student's *t*-test. $P < 0.05$ was considered statistically significant.

Acknowledgments

We thank Marie Iwado, Yoshiko Ueeda, Narumi Yamane and Takashi Nakamura for their technical assistance. We also thank Dr. Shinya Satoh for his helpful suggestions. This work was supported by Grants-in-Aid for Research on Hepatitis from the Ministry of Health, Labor, and Welfare of Japan; and by Japan Society for the Promotion of Science (JSPS) KAKENHI Grant no. 25293110.

Appendix A. Supplementary information

Supplementary data associated with this article can be found in the online version at http://dx.doi.org/10.1016/j.virol.2014.05.017.

References

Abe, K., Ikeda, M., Dansako, H., Naka, K., Kato, N., 2007. Cell culture-adaptive NS3 mutations required for the robust replication of genome-length hepatitis C virus RNA. Virus Res. 125, 88–97.

Ariumi, Y., Kuroki, M., Abe, K., Dansako, H., Ikeda, M., Wakita, T., Kato, N., 2007. DDX3 DEAD-box RNA helicase is required for hepatitis C virus RNA replication. J. Virol. 81, 13922–13926.

Ariumi, Y., Kuroki, M., Dansako, H., Abe, K., Ikeda, M., Wakita, T., Kato, N., 2008. The DNA damage sensors ataxia-telangiectasia mutated kinase and checkpoint kinase 2 are required for hepatitis C virus RNA replication. J. Virol. 82, 9639–9646.

Blight, K.J., McKeating, J.A., Rice, C.M., 2002. Highly permissive cell lines for subgenomic and genomic hepatitis C virus RNA replication. J. Virol. 76, 13001–13014.

Boulant, S., Douglas, M.W., Moody, L., Budkowska, A., Targett-Adams, P., McLauchlan, J., 2008. Hepatitis C virus core protein induces lipid droplet redistribution in a microtubule- and dynein-dependent manner. Traffic 9, 1268–1282.

Brasaemle, D.L., Dolios, G., Shapiro, L., Wang, R., 2004. Proteomic analysis of proteins associated with lipid droplets of basal and lipolytically stimulated 3T3-L1 adipocytes. J. Biol. Chem. 279, 46835–46842.

Choo, Q.L., Kuo, G., Weiner, A.J., Overby, L.R., Bradley, D.W., Houghton, M., 1989. Isolation of a cDNA clone derived from a blood-borne non-A, non-B viral-hepatitis genome. Science 244, 359–362.

Counihan, N.A., Rawlinson, S.M., Lindenbach, B.D., 2011. Trafficking of hepatitis C virus core protein during virus particle assembly. PLoS Pathog. 7, e1002302.

Dansako, H., Ikeda, M., Abe, K., Mori, K., Takemoto, K., Ariumi, Y., Kato, N., 2008. A new living cell-based assay system for monitoring genome-length hepatitis C virus RNA replication. Virus Res. 137, 72–79.

Dansako, H., Ikeda, M., Ariumi, Y., Wakita, T., Kato, N., 2009. Double-stranded RNA-induced interferon-beta and inflammatory cytokine production modulated by hepatitis C virus serine proteases derived from patients with hepatic diseases. Arch. Virol. 154, 801–810.

Dansako, H., Ikeda, M., Kato, N., 2007. Limited suppression of the interferon-beta production by hepatitis C virus serine protease in cultured human hepatocytes. FEBS J. 274, 4161–4176.

Dansako, H., Naganuma, A., Nakamura, T., Ikeda, F., Nozaki, A., Kato, N., 2003. Differential activation of interferon-inducible genes by hepatitis C virus core protein mediated by the interferon stimulated response element. Virus Res. 97, 17–30.

Dansako, H., Naka, K., Ikeda, M., Kato, N., 2005. Hepatitis C virus proteins exhibit conflicting effects on the interferon system in human hepatocyte cells. Biochem. Biophys. Res. Commun. 336, 458–468.

Dansako, H., Yamane, D., Welsch, C., McGivern, D.R., Hu, F.Y., Kato, N., Lemon, S.M., 2013. Class A scavenger receptor 1 (MSR1) restricts hepatitis C virus replication by mediating Toll-like receptor 3 recognition of viral RNAs produced in neighboring cells. PLoS Pathog. 9, e1003345.

Dejgaard, S.Y., Murshid, A., Erman, A., Kizilay, O., Verbich, D., Lodge, R., Dejgaard, K., Ly-Hartig, T.B., Pepperkok, R., Simpson, J.C., Presley, J.F., 2008. Rab18 and Rab43 have key roles in ER-Golgi trafficking. J. Cell Sci. 121, 2768–2781.

Hickenbottom, S.J., Kimmel, A.R., Londos, C., Hurley, J.H., 2004. Structure of a lipid droplet protein: the PAT family member TIP47. Structure 12, 1199–1207.

Hope, R.G., Murphy, D.J., McLauchlan, J., 2002. The domains required to direct core proteins of hepatitis C virus and GB virus-B to lipid droplets share common features with plant oleosin proteins. J. Biol. Chem. 277, 4261–4270.

Hutagalung, A.H., Novick, P.J., 2011. Role of Rab GTPases in membrane traffic and cell physiology. Physiol. Rev. 91, 119–149.

Ikeda, M., Abe, K., Dansako, H., Nakamura, T., Naka, K., Kato, N., 2005. Efficient replication of a full-length hepatitis C virus genome, strain O, in cell culture, and development of a luciferase reporter system. Biochem. Biophys. Res. Commun. 329, 1350–1359.

Ikeda, M., Abe, K., Yamada, M., Dansako, H., Naka, K., Kato, N., 2006. Different anti-HCV profiles of statins and their potential for combination therapy with interferon. Hepatology 44, 117–125.

Kato, N., 2001. Molecular virology of hepatitis C virus. Acta Med. Okayama 55, 133–159.

Kato, N., Mori, K., Abe, K., Dansako, H., Kuroki, M., Ariumi, Y., Wakita, T., Ikeda, M., 2009. Efficient replication systems for hepatitis C virus using a new human hepatoma cell line. Virus Res. 146, 41–50.

Kato, N., Sugiyama, K., Namba, K., Dansako, H., Nakamura, T., Takami, M., Naka, K., Nozaki, A., Shimotohno, K., 2003. Establishment of a hepatitis C virus sub-genomic replicon derived from human hepatocytes infected in vitro. Biochem. Biophys. Res. Commun. 306, 756–766.

Kenworthy, R., Lambert, D., Yang, F., Wang, N., Chen, Z., Zhu, Haizhen, Zhu, F., Liu, C., Li, K., Tang, H., 2009. Short-hairpin RNAs delivered by lentiviral vector transduction trigger RIG-I-mediated IFN activation. Nucleic Acids Res. 37, 6587–6599.

Mannova, P., Fang, R.H., Wang, H., Deng, B., McIntosh, M.W., Hanash, S.M., Beretta, L., 2006. Modification of host lipid raft proteome upon hepatitis C virus replication. Mol. Cell. Proteomics 5, 2319–2325.

Matto, M., Rice, C.M., Aroeti, B., Glenn, J.S., 2004. Hepatitis C virus core protein associates with detergent-resistant membranes distinct from classical plasma membrane rafts. J. Virol. 78, 12047–12053.

Miyanari, Y., Atsuzawa, K., Usuda, N., Watashi, K., Hishiki, T., Zayas, M., Bartenschlager, R., Wakita, T., Hijikata, M., Shimotohno, K., 2007. The lipid droplet is an important organelle for hepatitis C virus production. Nat. Cell Biol. 9, 1089–1097.

Ohkoshi, S., Kojima, H., Tawaraya, H., Miyajima, T., Kamimura, T., Asakura, H., Satoh, A., Hirose, S., Hijikata, M., Kato, N., Shimotohno, K., 1990. Prevalence of antibody against non-A, non-B hepatitis-virus in Japanese patients with hepatocellular-carcinoma. Jpn. J. Cancer Res. 81, 550–553.

Ohsaki, Y., Maeda, T., Maeda, M., Tauchi-Sato, K., Fujimoto, T., 2006. Recruitment of TIP47 to lipid droplets is controlled by the putative hydrophobic cleft. Biochem. Biophys. Res. Commun. 347, 279–287.

Ozeki, S., Cheng, J.L., Tauchi-Sato, K., Hatano, N., Taniguchi, H., Fujimoto, T., 2005. Rab18 localizes to lipid droplets and induces their close apposition to the endoplasmic reticulum-derived membrane. J. Cell Sci. 118, 2601–2611.

Salloum, S., Wang, H., Ferguson, C., Parton, R.G., Tai, A.W., 2013. Rab18 binds to hepatitis C virus NS5A and promotes interaction between sites of viral replication and lipid droplets. PLoS Pathog. 9, e1003513.

Shavinskaya, A., Boulant, S., Penin, F., McLauchlan, J., Bartenschlager, R., 2007. The lipid droplet binding domain of hepatitis C virus core protein is a major determinant for efficient virus assembly. J. Biol. Chem. 282, 37158–37169.

Shi, S.T., Lee, K.J., Aizaki, H., Hwang, S.B., Lai, M.M.C., 2003. Hepatitis C virus RNA replication occurs on a detergent-resistant membrane that cofractionates with caveolin-2. J. Virol. 77, 4160–4168.

Targett-Adams, P., Boulant, S., McLauchlan, J., 2008. Visualization of double-stranded RNA in cells supporting hepatitis C virus RNA replication. J. Virol. 82, 2182–2195.

The American Journal of Pathology, Vol. 184, No. 11, November 2014

The American Journal of
PATHOLOGY
ajp.amjpathol.org

GASTROINTESTINAL, HEPATOBILIARY, AND PANCREATIC PATHOLOGY

Hepatitis C Virus Core Protein Suppresses Mitophagy by Interacting with Parkin in the Context of Mitochondrial Depolarization

Yuichi Hara,* Izumi Yanatori,† Masanori Ikeda,‡ Emi Kiyokage,§ Sohji Nishina,* Yasuyuki Tomiyama,* Kazunori Toida,§ Fumio Kishi,† Nobuyuki Kato,‡ Michio Imamura,¶ Kazuaki Chayama,¶ and Keisuke Hino*

From the Departments of Hepatology and Pancreatology, Molecular Genetics,† and Anatomy,§ Kawasaki Medical School, Kurashiki; the Department of Tumor Virology,‡ Okayama University Graduate School of Medicine, Dentistry and Pharmaceutical Sciences, Okayama; and the Department of Gastroenterology and Metabolism,¶ Applied Life Sciences, Institute of Biomedical and Health Sciences, Hiroshima University, Hiroshima, Japan*

Accepted for publication July 25, 2014.

Address correspondence to Keisuke Hino, M.D., Ph.D., Department of Hepatology and Pancreatology, Kawasaki Medical School, 577 Matsushima, Kurashiki, Okayama 701-0192, Japan. E-mail: khino@med.kawasaki-m.ac.jp.

Hepatitis C virus (HCV) causes mitochondrial injury and oxidative stress, and impaired mitochondria are selectively eliminated through autophagy-dependent degradation (mitophagy). We investigated whether HCV affects mitophagy in terms of mitochondrial quality control. The effect of HCV on mitophagy was examined using HCV-Japanese fulminant hepatitis-1–infected cells and the uncoupling reagent carbonyl cyanide *m*-chlorophenylhydrazone as a mitophagy inducer. In addition, liver cells from transgenic mice expressing the HCV polyprotein and human hepatocyte chimeric mice were examined for mitophagy. Translocation of the E3 ubiquitin ligase Parkin to the mitochondria was impaired without a reduction of pentaerythritol tetranitrate–induced kinase 1 activity in the presence of HCV infection both *in vitro* and *in vivo*. Coimmunoprecipitation assays revealed that Parkin associated with the HCV core protein. Furthermore, a Yeast Two-Hybrid assay identified a specific interaction between the HCV core protein and an N-terminal Parkin fragment. Silencing Parkin suppressed HCV core protein expression, suggesting a functional role for the interaction between the HCV core protein and Parkin in HCV propagation. The suppressed Parkin translocation to the mitochondria inhibited mitochondrial ubiquitination, decreased the number of mitochondria sequestered in isolation membranes, and reduced autophagic degradation activity. Through a direct interaction with Parkin, the HCV core protein suppressed mitophagy by inhibiting Parkin translocation to the mitochondria. This inhibition may amplify and sustain HCV-induced mitochondrial injury. *(Am J Pathol 2014, 184: 3026–3039; http://dx.doi.org/10.1016/j.ajpath.2014.07.024)*

Oxidative stress is present in chronic hepatitis C to a greater degree than in other inflammatory liver diseases.[1,2] The hepatitis C virus (HCV) core protein induces the production of reactive oxygen species (ROS)[3,4] through mitochondrial electron transport inhibition.[5] Because the mitochondria are targets for ROS and ROS generators, HCV-induced ROS have the potential to injure mitochondria. In addition, hepatocellular mitochondrial alterations have been observed in patients with chronic hepatitis C.[6] We previously identified a ROS-associated iron metabolic disorder[7] and demonstrated that transgenic mice expressing the HCV polyprotein develop hepatocarcinogenesis related to mitochondrial injury induced by HCV and iron overload.[8] Therefore, impaired mitochondrial function may play a critical role in the development of hepatocellular carcinoma (HCC) in patients with chronic HCV infection. Conversely, the affected mitochondria are selectively eliminated through the autophagy-dependent degradation of mitochondria (referred to as mitophagy) in both physiological and pathological settings to maintain the mitochondrial quality.[9,10] On the

Supported by Japan Society for the Promotion of Science Grant-in-Aid for Scientific Research (B) 23390201 and Grant-in-Aid for Exploratory Research 25670374; Ministry of Health, Labor and Welfare of Japan Health and Labor Sciences Research grant 25200601 for research on hepatitis; and Kawasaki Medical School Research Project grant P2.

Disclosures: None declared.

Current address of M.I., Kagoshima University Graduate School of Medical and Dental Sciences, Kagoshima, Japan.

http://dx.doi.org/10.1016/j.ajpath.2014.07.024

basis of these observations, we hypothesized that HCV may suppress mitophagy, which could lead to the sustained presence of affected mitochondria, increased ROS production, and the development of HCC.

Mitochondrial membrane depolarization precedes mitophagy induction,[11] which is selectively controlled by a variety of proteins in mammalian cells, including pentaerythritol tetranitrate–induced kinase 1 (PINK1) and the E3 ubiquitin ligase Parkin.[12–19] PINK1 facilitates Parkin targeting of the depolarized mitochondria.[12–15] Although Parkin ubiquitinates a broad range of mitochondrial outer membrane proteins,[14,17–19] it remains unclear how Parkin enables the damaged mitochondria to be recognized by the autophagosome. Structures containing autophagy-related protein 9A and the uncoordinated family member-51–like kinase 1 complex independently target depolarized mitochondria at the initial stages of Parkin-mediated mitophagy, whereas the autophagosomal microtubule-associated protein light chain 3 (LC3) is critical for efficient incorporation of damaged mitochondria into the autophagosome at a later stage.[20] LC3-I undergoes post-translational modification by phosphatidylethanolamine to become LC3-II, and LC3-II insertion into the autophagosomal membrane is a key step in autophagosome formation. In addition, the autophagic adaptor p62 is recruited to mitochondrial clusters and is essential for mitochondrial clearance,[13] although it remains controversial as to whether p62 is essential for mitochondrial recognition by the autophagosome[13] or rather is important for perinuclear clustering of depolarized mitochondria.[19,21] Our aim was to examine whether HCV suppresses mitophagy. We found that HCV core protein inhibits the translocation of Parkin to affected mitochondria by interacting with Parkin and subsequently suppressing mitophagy. These results imply that mitochondria affected by HCV core protein are unlikely to be eliminated, which may intensify oxidative stress and increase the risk of hepatocarcinogenesis.

Materials and Methods

Cell Culture, HCV Infection Experiments, and Mitochondrial Depolarization

HCV-Japanese fulminant hepatitis-1 (JFH1)–infected Huh7 cells have previously been described in detail.[22] The supernatants were collected from cell culture–generated JFH1-Huh7 cells at 21 days after infection and stored until use at −80°C after filtering through a 0.45-μm filter. For infection experiments with the HCV-JFH1 virus, 1×10^5 Huh7 cells per well were plated onto 6-well plates and cultured for 24 hours. Then, we infected the cells with 50 μL (equivalent to a multiplicity of infection of 0.1) of inoculum. The culture supernatants were collected, and the levels of the HCV core were determined using an enzyme-linked immunosorbent assay (ELISA; Mitsubishi Kagaku Bio-Clinical Laboratories, Tokyo, Japan). Total RNA was isolated from the infected cellular lysates using an RNeasy mini kit (Qiagen, Hilden, Germany) for quantitative RT-PCR analysis of the intracellular HCV RNA. The HCV infectivity in the culture supernatants was determined by a focus-forming assay at 48 hours after infection. The HCV-infected cells were detected using an anti-HCV core antibody (CP-9 and CP-11, Institute of Immunology, Ltd, Tokyo, Japan). Intracellular HCV infectivity was determined using a focus-forming assay at 48 hours after inoculation of the lysates by repeated freeze-and-thaw cycles (three times).

To depolarize the mitochondria, the cells were treated with 10 μmol/L carbonyl cyanide *m*-chlorophenylhydrazone (CCCP; Sigma-Aldrich, St. Louis, MO) for 1 to 2 hours or 1 μmol/L valinomycin (Sigma-Aldrich) for 3 hours; CCCP represses ATP synthesis through the loss of the H^+ gradient without affecting mitochondrial electron transport, which is known to induce mitochondrial fragmentation.[13]

Animals

The pAlbSVPA-HCV vector, which contains the full-length polyprotein-coding region under the control of the murine albumin promoter/enhancer, has previously been described in detail.[23,24] Of the four transgenic lineages with evidence of RNA transcription of the full-length HCV-N open reading frame (FL-N), the FL-N/35 lineage proved capable of breeding large numbers.[24] Urokinase-type plasminogen activator–transgenic severe combined immunodeficiency mice were generated, and human hepatocytes were transplanted to generate chimeric mice.[25] The chimeric mice were injected with genotype *1b* HCV-positive human serum samples, as described previously.[26] The mouse livers were extracted 12 weeks after the infection, when the serum HCV RNA titers had increased over baseline levels. Male FL-N/35 transgenic mice, age-matched C57BL/6 mice (control), and chimeric mice with and without HCV infection were fed, maintained, and then euthanized by i.p. injection of 10% nembutal sodium, according to the guidelines approved by the Institutional Animal Care and Use Committee. The study protocol for obtaining human serum samples conformed to the ethical guidelines of the 1975 Declaration of Helsinki and was approved by the Institutional Review Committee.

Measurement of HCV RNA and Human Albumin in the Serum of Chimeric Mice

HCV RNA[26] and human albumin[25] were quantified as described previously. Human albumin levels in the serum of chimeric mice were determined using the Human Albumin ELISA Quantification kit (Bethyl Laboratories Inc., Montgomery, TX).

Measurement of Mitochondrial Membrane Potential

The mitochondrial membrane potential ($\Delta\Psi$) was measured using a Cell Meter JC-10 Mitochondrial Membrane Potential Assay kit (AAT Bioquest, Inc., Sunnyvale, CA), according to the manufacturer's instructions. The fluorescent intensities

for both J-aggregates (red) and monometric forms (green) of JC-10 were measured at Ex/Em = 490/525 nm and 540/590 nm with a Varioskan Flush Multimode Reader (Thermo Fisher Scientific, Waltham, MA).

Isolation of Mitochondria

The cells were lysed by mechanical homogenization using a small pestle, and mitochondrial extraction was performed using a Qproteome Mitochondria Isolation kit (Qiagen), according to the manufacturer's instructions. Liver mitochondria were isolated as described previously with some modifications.[27] In brief, the livers were minced on ice and homogenized by five strokes with a Dounce homogenizer and a tight-fitting pestle in isolation buffer [70 mmol/L sucrose, 1 mmol/L KH_2PO_4, 5 mmol/L HEPES, 220 mmol/L mannitol, 5 mmol/L sodium succinate, and 0.1% bovine serum albumin (BSA), pH 7.4]. The homogenate was centrifuged at 800 × *g* for 5 minutes at 4°C. The supernatant fraction was retained, whereas the pellet was washed with isolation buffer and centrifuged again. The combined supernatant fractions were centrifuged at 1000 × *g* for 15 minutes at 4°C to obtain a crude mitochondrial pellet.

Measurement of ROS

The cellular ROS level was measured by oxidation of the cell-permeable, oxidation-sensitive fluorogenic precursor, *2′,7′*-dihydrodichlorofluorescein diacetate (Molecular Probes Inc., Eugene, OR). Fluorescence was measured using a Varioskan Flush Multimode Reader at 495/535 nm (excitation/emission).

Determination of Glutathione Content

Mitochondrial pellets were measured for total glutathione [reduced glutathione (GSH) + oxidized glutathione (GSSG)] and GSH content using the GSSG/GSH Quantification kit (Dojindo Molecular Technologies, Inc., Kumamoto, Japan). The concentration of GSH was calculated using the following formula:

$$\text{GSH concentration} = \text{Total glutathione concentration} - [\text{GSSG concentration}] \times 2 \quad (1)$$

The liver tissue samples (approximately 50 mg) were minced in ice-cold metaphosphoric acid solution, homogenized, and centrifuged at 3000 × *g* for 10 minutes at 4°C. Lysates from the liver tissue samples and mitochondrial samples (2 mg) were evaluated for the concentration of GSH using the thioester method and a GSH-400 kit (Oxis International Inc., Portland, OR) and for total glutathione content using the glutathione reductase–dinitrothiocyanobenzene recycling assay and the GSH-412 kit (Oxis International Inc.), as described previously.[5]

Immunoblotting

Samples were lysed in radioimmunoprecipitation assay buffer [20 mmol/L Tris-HCl (pH 7.5), 150 mmol/L NaCl, 50 mmol/L NaF, 1 mmol/L Na_3VO_4, 0.1% SDS, and 0.5% Triton X-100], as described previously,[28] supplemented with 1% protease inhibitor mixture (Sigma-Aldrich) and 100 mmol/L phenylmethylsulfonyl fluoride. Cell lysates or mitochondrial pellets were subjected to immunoblot analysis using an iBlot Gel Transfer Device (Invitrogen, Carlsbad, CA). The membranes were incubated with the following primary antibodies: rabbit anti-human LC3 (Novus Biologicals, Littleton, CO), rabbit anti-human p62/SQSTM1 (MBL, Nagoya, Japan), rabbit anti-human Parkin (Cell Signaling Technology, Danvers, MA), mouse anti-human Parkin (Santa Cruz Biotechnology, Inc.), rabbit anti-human p-Parkin (Ser 378; Santa Cruz Biotechnology, Inc.), rabbit anti-human PINK1 (Cell Signaling Technology), mouse anti-human mitochondrial heat shock protein-70 (BioReagents, Golden, CO), mouse anti-human ubiquitin (Santa Cruz Biotechnology, Inc.), goat anti-human voltage-dependent anion-selective channel protein 1 (VDAC1; Santa Cruz Biotechnology, Inc.), monoclonal antisynthetic HCV core peptide (CP11; Institute of Immunology, Ltd), mouse anti-HCV non-structural (NS) 3 protein (Abcam, Cambridge, MA), mouse anti-HCV NS4A (Abcam), mouse anti-HCV NS5A protein (Abcam), and rabbit anti-human β-actin (Cell Signaling Technology).

Electron Microscopy

To address the detail localization of core and Parkin, the cells treated with CCCP for 1 hour were fixed with 4% paraformaldehyde and 1% glutaraldehyde in 0.1 mol/L Millonig's phosphate buffer (pH 7.4) for 30 minutes. The cells were incubated with a mixture of the following primary antibodies in phosphate-buffered saline (PBS) containing 1% BSA and 0.05% sodium azide overnight at 20°C: mouse monoclonal antisynthetic HCV core peptide (Institute of Immunology), rabbit anti-human Parkin (Abcam), and rabbit anti-rat LC3 (Wako Pure Chemical Industries, Ltd, Osaka, Japan). After washing with PBS, the cells were incubated with biotinylated donkey anti-rabbit IgG (Jackson ImmunoResearch Laboratories, Inc., Baltimore Pike, PA) in 1% BSA for 2 hours at 20°C. After washing with PBS, the cells were incubated with Alexa Fluor-488 FluoroNanogold-streptavidin (Jackson ImmunoResearch Laboratories, Inc.), indocarbocyanine-labeled donkey anti-mouse IgG (Jackson ImmunoResearch Laboratories, Inc.), and indocarbocyanine-labeled donkey anti-rabbit IgG (Jackson ImmunoResearch Laboratories, Inc.) in 1% BSA for 2 hours at 20°C. After washing with PBS, the cells were incubated with mouse peroxidase–anti-peroxidase complex (Jackson ImmunoResearch Laboratories, Inc.) in PBS for 3 hours at 20°C. The peroxidase reduction was developed with 0.05% diaminobenzidine tetrahydrochloride in 50 mmol/L Tris buffer containing 0.01% hydrogen peroxide for 20 minutes at room temperature. The diameter of the gold immunoparticles was increased using a silver enhancement kit (HQ silver; Nanoprobes, Inc., Yaphank, NY) for 4 minutes at